

PAPER

[View Article Online](#)
[View Journal](#) | [View Issue](#)Cite this: *J. Mater. Chem. B*, 2025,
13, 11855

Evaluation of peripheral analgesia in a rat incisional pain model using degradable hydrophilic microspheres for sustained delivery of buprenorphine

Laurent Bédouet,^a Anne Beilvert,^a Emeline Servais,^a Florentina Pascale,^b Saïda Homayra Ghegediban,^b Michel Wassef,^c Julien Namur^b and Laurence Moine^d *^d

To target peripheral opioid receptors for postoperative pain relief while minimizing systemic opioid side effects, low doses of buprenorphine hydrochloride (0.8 up to 4.8 mg mL⁻¹) were loaded into prefabricated, hydrophilic, degradable polyethylene glycol-based microspheres (PEG-MS, 50–100 μm) used as a drug delivery platform. By varying the composition of the degradable crosslinker, the degradation rate of PEG-MS, and consequently the drug release duration, could be tuned from 2 days to 2 months. In a pharmacokinetic study in rabbits, the time to the last quantifiable serum concentration (T_{last}) of buprenorphine increased with the degradation time of PEG-MS, reaching 1, 2, 4, and 7 days for microspheres degrading over 2, 6, 12, and 50 days, respectively. PEG-MS demonstrated good biocompatibility, as evidenced by only mild and transient local inflammatory responses during their degradation when implanted in various rabbit tissues, including the dermis, muscle, and subconjunctival space. In a rat incisional pain model, the intraplantar injection of buprenorphine-loaded PEG-MS (degrading over 12 days) at doses of 240 μg and 40 μg increased the paw withdrawal threshold at 24 h by 34% ($p < 0.0001$) and 20% ($p = 0.0466$), respectively, compared to drug-free microspheres. Serum concentrations of buprenorphine exceeded the therapeutic threshold, indicating that intraplantar administration resulted in systemic, rather than local, effects. In the context of the opioid crisis, the local administration of a degradable drug delivery system that releases a small amount of buprenorphine in an operative wound for a few days after surgery seems relevant. Nevertheless, while the PEG-MS as buprenorphine delivery system was effective, this preliminary study showed that their local administration resulted in the opioid spreading throughout the body. The future of peripheral analgesia lies in developing opioids with physicochemical properties that prevent them from reaching the brain or being active there.

Received 2nd June 2025,
Accepted 18th August 2025

DOI: 10.1039/d5tb01312g

rsc.li/materials-b

Introduction

Each year, 310 million surgical procedures are performed worldwide. A significant proportion of patients (≈80%) experiences undesirable levels of postoperative pain in the first 24 h.^{1,2} The intensity and duration of this acute pain can increase the risk of developing chronic or persistent postsurgical pain, which affects between 10% to 30% of cases.³ Such

long-term pain can lead to serious psychological, social, and economic consequences. For this reason, effective management of acute postoperative pain is essential to improve patient outcomes.

Buprenorphine exhibits unique pharmacological properties compared to other opioids as a partial μ receptor agonist, *i.e.*, it binds strongly to the receptors without fully activating them, providing a therapeutic effect with fewer side effects.^{4–6} Its activity in postoperative pain management has been documented in various reviews,^{7,8} demonstrating effectiveness with a relatively low side effect profile. The analgesic effects typically last around 6 hours. The main side effect of buprenorphine is respiratory depression.⁹

To reduce the potential side effect of opioids, local injection of low dose of opioids directly in tissues after the surgery could

^a Occlugel, 17 bis, avenue des Andes, 91940 Les Ulis, France^b Archimmed, 17 bis, avenue des Andes, 91940 Les Ulis, France^c Université René Diderot, Department of Pathology, APHP, Hôpital Lariboisière, 2 rue Ambroise Paré, 75010 Paris, France^d Université Paris-Saclay, CNRS, Institut Galien Paris-Saclay, 17 avenue des Sciences, 91400 Orsay, France. E-mail: laurence.moine@universite-paris-saclay.fr

provide significant pain reduction for 6–8 h.¹⁰ The rationale is based on the discovery of functional opioid receptors on the peripheral nerve endings of the nociceptors.^{11,12} Indeed, peripheral opioid receptors located in the skin,¹³ joints,¹⁴ cornea,¹⁵ sciatic nerve^{16,17} and viscera¹⁸ can be targeted for effective analgesia without the central effects associated with systemic opioid treatment. Local delivery of opioids in wounded tissues after surgery represents a promising strategy to inhibit the pain at its source.¹⁹ The peripheral opioid system allows the development of novel pain treatment strategies by separating analgesic action from unwanted central side effects.²⁰ Different solutions for peripheral analgesia are being investigated, such as the development of new opioid drugs with low brain diffusion¹⁹ or drug delivery systems (DDS) for local delivery of opioids to peripheral tissues.²¹ However, the analgesic effect of peripherally administered opioids in the postoperative setting is often short-lived,¹⁰ likely due to rapid tissue clearance and drainage of the locally applied drugs.

In this study, we explored the promising strategy of achieving peripheral analgesia through the local, sustained release of low doses of buprenorphine from a degradable DDS. This approach involves the local postoperative injection of the DDS to gradually activate peripheral opioid receptors and prolong postoperative analgesia. Sustained delivery products containing buprenorphine are already marketed as implants for the treatment of opioid dependence of patients. In this indication, intramuscular implants (Probuphine[®]/Sixmo[®], Buvidal[®], Sublocade[®]) provide for several weeks stable plasmatic concentrations of buprenorphine.²² However, these implants are not compatible with surgical wounds infiltration either because they are non-degradable (Probuphine[®]/Sixmo[®]) or contain organic solvents (*N*-methyl-pyrrolidone for Sublocade[®] and ethanol for Buvidal[®]).

To address this limitation, we developed a particular composition of biocompatible and biodegradable microspheres (PEG-MS), consisting of poly(ethylene glycol) hydrogel cross-linked with a hydrolyzable crosslinker as platform delivery of buprenorphine. Originally designed for embolization²³ and chemoembolization,^{24,25} PEG-MS were adapted to load small quantities of buprenorphine and engineered to degrade at controlled rates. The goal was to achieve local therapeutic effect over the critical 3-day postoperative pain period, while minimizing systemic exposure to reduce the risk of opioid side effects. The release kinetics of buprenorphine were evaluated *in vitro* and *in vivo* following a single subcutaneous injection in rabbits, aiming to identify a formulation capable of maintaining drug release for at least 3 days *in vivo*. The biocompatibility of the PEG-MS was evaluated by histology in various rabbit tissues. To evaluate analgesic efficacy, buprenorphine-loaded

PEG-MS were administered by intraplantar injection in the Brennan model of postoperative pain in rats to investigate the anti-allodynic effect over 3 days.

Methods

Preparation and characterization of PEG-MS

Material. Poly(ethylene glycol) methyl ether methacrylate (PEGma) ($M_n = 300 \text{ g mol}^{-1}$), poly(ethylene glycol), $M_n = 600 \text{ g mol}^{-1}$, ϵ -caprolactone (Cl), stannous 2-ethylhexanoate, methacrylic anhydride, phosphate buffer solution (PBS), 2,2'-azobis(2-methylpropionitrile) and buprenorphine hydrochloride (PHR1729-50MG) were purchased from Sigma-Aldrich France. DL-Lactide was purchased from polysciences.

PEG-MS synthesis. Polyethyleneglycol-based degradable microspheres for buprenorphine delivery (PEG-MS) were synthesized by suspension polymerization.²³ By varying the composition of the degradable crosslinker described in patents,^{26,27} four microspheres with different degradation times ranging from two days up to two months were obtained (Table 1 and Table S1). These microspheres are designated PEG-MS2, PEG-MS6, PEG-MS12, and PEG-MS50, corresponding to their respective degradation times of 2, 6, 12, and 50 days. Briefly, the degradable crosslinkers (PEG₁₃-LA₁₂, PEG₁₃-LA₈-co-Cl₂, PEG₁₃-LA₇-co-Cl₃ and PEG₁₃-LA₄-co-Cl₅) have been synthesized by polymerization of polyethylene glycol, $M_n = 600 \text{ g mol}^{-1}$ with DL-lactide and ϵ -caprolactone with stannous 2-ethylhexanoate during 20 h at 115 °C. After polymerization and precipitation, the end chain functionalization was done with methacrylic anhydride at 80 °C for 8 h. Polymerization suspension was done with dimethacrylate derivatives of crosslinker and polyethylene glycol methyl ether methacrylate (PEGma) at 80 °C during 8 h in presence of 2,2'-azobis(2-methylpropionitrile). Then, PEG-MS were collected by filtration on a 40 μm sieve and washed extensively with acetone and water. Microspheres were then sieved with decreasing size of sieves (315, 100 and 50 μm) and the fraction 50–100 μm was collected for the buprenorphine delivery study.

Optical sizing of PEG-MS. After sieving, the PEG-MS were poured into a Petri dish and pictures were taken with an optical microscope at 10 \times magnification (Leitz, Diaplan) equipped with a digital camera (Allied Vision Mako). Microspheres diameter was determined with the Image J software (100 measures).

Dry weight determination of PEG-MS. In triplicate, after the sieving step 1 ml of wet PEG-MS was placed in pre-weighed 15 ml polypropylene vials before freeze-drying. Then, the dry microsphere weight was determined by weighing.

Loading of buprenorphine. After the sieving step, 1 mL of microspheres was placed in 15 mL polypropylene vials in 3 mL

Table 1 PEG-MS used for buprenorphine sustained release experiments

	PEG-MS2	PEG-MS6	PEG-MS12	PEG-MS50
Degradable crosslinker composition	PEG ₁₃ -LA ₁₂	PEG ₁₃ -LA ₈ -co-Cl ₂	PEG ₁₃ -LA ₇ -co-Cl ₃	PEG ₁₃ -LA ₄ -co-Cl ₅
<i>In vitro</i> degradation time	2 days	6 days	12 days	2 months



of water before mixing with buprenorphine hydrochloride (1 mg, 4 mg, 5 mg). The loading step was done at room temperature for 2 h under stirring on a tube rotator (≈ 30 rpm). Then, the supernatants were removed for the measurement of unbound buprenorphine hydrochloride by fluorimetry (λ_{ex} 280 nm, λ_{em} 354 nm, Hitachi F2000). The amount of buprenorphine in supernatant was obtained by extrapolation from a standard curve (0.6 to 25 $\mu\text{g mL}^{-1}$). The loaded dose was calculated by subtracting the final amount of buprenorphine from the initial amount. The loading efficiency was calculated by the following equation: loading efficiency = ((buprenorphine in feed – buprenorphine in supernatant)/buprenorphine in feed) \times 100. The amount of buprenorphine loaded onto microspheres was given in mg per mL of MS (mg mL^{-1}) as is common in chemoembolization for the quantification of anticancer agents loaded onto the drug eluting beads,^{28,29} but also in percentage of dry weight (w/w): drug loading = (mg of buprenorphine loaded onto 1 mL of microsphere)/(dry weight (mg) of 1 mL of drug-free microsphere) \times 100. Then, the microsphere pellets were freeze-dried (Christ, Alpha 2-4 LSC basic) at 0.2 mbar and -80°C during 4–5 days in the dark. Samples were exposed to e-beam radiation at room temperature and air atmosphere in a linear electron accelerator. The electrons emitted have a single energy level of $9.8 \text{ MeV} \pm 0.2$, and the passage speed was adjusted to deliver a dose of 25 kGy (Ionisos, Chaumesnil, France).

In vitro drug release study. PBS (25 mL) prewarmed at 37°C was added to the dry and sterile microspheres loaded with buprenorphine, and the tubes were placed horizontally in an orbital shaker (IKA) at 37°C under shaking (150 rpm). Samples were removed at 10 min, 5 h and every day until degradation of microspheres. At each sampling time, all medium was totally renewed. The amounts of free buprenorphine in PBS supernatants were determined by fluorimetry (λ_{ex} 280 nm, λ_{em} 354 nm, Hitachi F2000) as described above. Blank (drug free) PEG-MS were incubated under the same conditions to exclude interference from PEG-MS degradation products on the buprenorphine fluorimetric assay.

Degradation rate of sterile PEG-MS during buprenorphine release. PEG-MS degradation was monitored during buprenorphine release using a colorimetric assay as previously described.³⁰ The PEGylated degradation products released into PBS during the time were quantified using an iodine and barium assay.³¹ Standard curves (5 μg up to 25 μg) were prepared using a solution of PEG-MS degradation products diluted in PBS at 1 mg mL^{-1} . Absence of buprenorphine interference in the colorimetric assay of PEGylated products was verified.

Animal studies

For the pharmacokinetic and the biocompatibility studies, experiments were conducted in accordance with the French regulation regarding experiments conducted on live animals (Directive 2010/63/EU of the European Parliament). For the anti-allodynic study, rats were treated according to the

guidelines of the Committee for Research and Ethical Issue of the I.A.S.P. (1983) and the European guidelines 2010/63/UE.

Labelling of mu receptors in the plantar aspect of the foot in rat. Rat paws were thawed directly in alcohol formalin glacial acetic fixative and then demineralized for 3 days. Then, sagittal sections of plantar aspect of the foot were performed. After dehydration in successive baths of ethanol, acetone and xylene, samples were embedded in paraffin. After deparaffinization of sections (5 μm), antigenic sites were unmasked by citrate/microwave pretreatment for 10 min, before overnight incubation at 4°C with rabbit anti-mu opioid receptor antibody (Abcam, ab217766) at dilution 1:100 in PBS-BSA 3%. After inhibition of endogenous peroxidases by hydrogen peroxide, the sections were incubated in the peroxidase-coupled secondary antibody (Dako, Envision rabbit, ref. K4002). Reaction with diaminobenzidine (Dako, ref. K3468) revealed antigen-antibody complexes by the appearance of a brown staining. Sections were counterstained with Mayer's hematoxylin, then mounted between slide and coverslip in aqueous medium. As negative control, the primary antibody was replaced by PBS-BSA 3%.

Pharmacokinetic study in rabbit. The procedures were submitted to the “Comité d’Ethique en matière d’Expérimentation Animale Anses/ENVA/UPEC (C2EA16)” under number 17-029 and received a positive notification from the “Ministère de l’Enseignement Supérieur, de la Recherche et de l’Innovation” on January 24, 2019. Injectable buprenorphine (Bupaq[®], Multi-dose 0.3 mg mL^{-1} Injectable solution, Virbac, France) was administrated at the dose of $30 \mu\text{g kg}^{-1}/12 \text{ h}$ as reference, and sterile PEG-MS degradable in 2, 6, 12 and 50 days loaded with buprenorphine were implanted subcutaneously in the back behind the neck of 5 male New-Zealand rabbits ($4.35 \pm 0.4 \text{ kg}$ – min–max $4.05\text{--}4.95 \text{ kg}$) with a 23G needle in a 3 mL syringe (Medaillon[®], Merit Medical) (Table S2). The dose of buprenorphine injected for the PEG-MS was determined as the dose equivalent to repeated injectable buprenorphine injections over the period of buprenorphine elution from PEG-MS determined *in vitro*, i.e. for a delivery of 10 days, the total dose injected with injectable buprenorphine was $60 \mu\text{g kg}^{-1} \text{ day}^{-1}$ per injection \times 10 injections. Blood samples ($\sim 2.5 \text{ mL}$) were through the auricular artery to assess the systemic concentration of buprenorphine at the following time points: pre-injection (T0), 15 min, 30 min, 1 h, 3 h, 5 h, 24 h, 2 D, 4 D, 7 D, 14 D, 21 D, 28 D. Buprenorphine quantifications were done by coupled HPLC-MS/MS (SI1). Statistical analysis of the data was not performed owing to the small number of animals treated. This study was designed to determine whether buprenorphine loading onto the PEG-MS would extend its delivery time in serum compared to free buprenorphine.

Pharmacokinetic data analysis. Results from each rabbit were grouped according to products and the blood collection time point. The serum concentration of buprenorphine was plotted for the time points to generate serum concentration–time curves, which were compared between injectable (free) buprenorphine and PEG-MS groups. Pharmacokinetic parameters were calculated using a non-compartmental analysis



that assumed a total-body exposure to the drug. Calculated parameters, including maximal observed serum concentration (C_{\max}), time to maximal observed serum concentration, (T_{\max}), time to the last quantifiable serum buprenorphine concentration (T_{last}), terminal elimination half-life ($t_{1/2}$), area under the curve ($\text{AUC}_{0-T_{\text{last}}}$) from time 0 to T_{last} were determined from the individual observed concentration time data. $\text{AUC}_{0-T_{\text{last}}}$ was obtained by calculation of the area under the concentration curve by the trapezoid method using the equation: $S = ((C_1 + C_2)/2) \times (T_2 - T_1)$, and the terminal half-life ($t_{1/2}$) by dividing the natural logarithm of 2 with the elimination slope ($K_e = \ln C_1 - \ln C_2 / T_2 - T_1$) found by graphic analysis with 2 time points on the terminal portion of the serum curves by determining on the ordinate axis the time interval elapsed between the concentration C and the concentration $C/2$.

Rabbit biocompatibility study of blank PEG-MS12 in dermis, muscle and subconjunctival space. The procedures were submitted to the “Comité d’Ethique en matière d’Expérimentation Animale Anses/ENVA/UPEC (C2EA16)” under identification number #17-029 on October 12, 2018, and received a positive notification from the “Ministère de l’Enseignement Supérieur, de la Recherche et de l’Innovation” on January 24, 2019. Male white New Zealand rabbits (3.92 ± 0.19 kg – min–max 3.54–4.26 kg, $n = 12$) were treated with an anti-infective drug (Trisulmix[®], trimetoprim and sulphadimethoxine, 0.2 mL kg^{-1} in drinking water daily), starting the day of injection until the day of sacrifice, and with antibiotic (enrofloxacin 2.5% , $7.5 \text{ mg kg}^{-1} \text{ day}^{-1}$ injected subcutaneously for 7 days after implantation). Lighting was automatically controlled for approximately 12 h per day. Anesthesia was performed by intramuscular injection of 10 mg kg^{-1} ketamine and 2.5 mg kg^{-1} xylazine and maintained with oxygen (100%) and isoflurane (1 to 3%) delivered through supraglottic airway device. Animals were placed in dorsal decubitus. Analgesia was done by intramuscular injection of 0.1 mL kg^{-1} buprenorphine (Vetergesic) at the end of the procedure. A vascular access was gained in the auricular vein and artery for perfusion and blood sample respectively. Details of microsphere implantation and histology work are given in the SI2.

Incisional pain model. The standard protocol describing the animal model used in this study was approved by the Animal Ethical Committee (Comité d’Ethique pour l’Expérimentation Animale Auvergne – C2E2A) and accredited by the “Ministère de l’Enseignement Supérieur, de la Recherche et de l’Innovation” under national authorisation number #11887. Thirty male Sprague-Dawley rats (SPF status, Janvier, France), weighing 188–234 g the day of surgery were used in the pharmacodynamic part, and 6 males (205–225 g) the day of treatment were used in the pharmacokinetic study (satellite group). Briefly, rats were housed at $20\text{--}24^\circ\text{C}$ and relative humidity ($45\text{--}65\%$) controlled room and acclimated to an artificial day/night cycle of 12 h light/12 h darkness. Rats had free access to tap water and were fed *ad libitum* with pelleted complete diet. Animals were housed 3 or 4 per cage (type E) and were acclimated for a period of at least 5 days before any testing. Surgery was done under gas anaesthesia (2.5% isoflurane/ 3 L min^{-1}). For all rats,

the plantar aspect of the left hindpaw was exposed and a 1 cm longitudinal incision was made using a surgical blade, through skin and fascia of the plantar aspect of the foot, starting 0.5 cm from the proximal edge of the heel and extending toward the toes. The plantaris muscle was elevated and incised longitudinally whereas the insertions remained intact. After haemostasis with gentle pressure, the skin was stitched up with three sutures.³²

Intraplantar injection of PEG-MS preloaded with buprenorphine. After surgery (D0) right after completion of the surgical procedure, $100 \mu\text{L}$ suspension of PEG-MS in water (ratio 1/1) was intraplantarly administered at 3 different doses of buprenorphine (blank PEG-MS/BU1/BU2): $0/240 \mu\text{g}$ (buprenorphine loading at 4.8 mg mL^{-1})/ $40 \mu\text{g}$ (buprenorphine loading at 0.8 mg mL^{-1})/animal. For practical reasons, dosing was done group by group in a non-random order, which could introduce a potential risk of bias. The low dose ($40 \mu\text{g}$) was arbitrarily chosen given the wide range of buprenorphine concentrations that can be administered subcutaneously in rats, from 5 to $500 \mu\text{g kg}^{-1}$.^{33,34} The high dose ($240 \mu\text{g}$) corresponded to the dose commonly used for post-operative pain control in animals treated with buprenorphine extended-release formulations, *i.e.* a final dose of 1.2 mg kg^{-1} on a body weight basis^{35–39} (based on an average rat weight of 200 g). A buprenorphine loading of PEG-MS12 at 4.8 mg mL^{-1} was selected to achieve this dosing allowing the administration of $50 \mu\text{L}$ of pellet (Table S3). PEG-MS12 were injected at surgery site under gas anaesthesia with a 23G needle attached to a 1 mL Luer syringe (Medaillon[®], Merit Medical) inserted approximately 1 cm rostrally to the skin surgical incision and pushed parallel to the skin to the rear limit of the incision. The tip of the needle should be placed in the incised muscle. The target dose was then administered by retroinjection along the surgical incision, while compression was maintained on the incision site with the thumb to avoid leakage.

Assessment of the anti-allodynic effect of PEG-MS12 and blood sampling. On D1, D2, and D3 after surgery paw withdrawal threshold was measured using the electronic Von Frey (EVF3 model, Bioseb, France). Each reaction threshold measure was repeated three times for both hindpaws (operated and unoperated) with intervals of approximately 2–3 min. Allodynia testing was performed in a random order by a blinded experimenter. For blood sampling at D3, serum samples from three randomly chosen rats in the groups BU1 and BU2 were collected by intra-cardiac puncture. Serum samples were also collected in the satellite group ($n = 6$) at 24 h and 48 h after wound infiltration with PEG-MS12 loaded with buprenorphine. Briefly, animals were anaesthetized (3% isoflurane, 3 L min^{-1}) and 1.0 mL of blood was collected in the caudal vein. Samples were gently mixed and were placed in ice and centrifuged at the latest within 30 min after collection at 4600 rpm for 5 min at room temperature. Serum samples were gently collected and frozen immediately (-80°C). Rats were sacrificed at the end of the experiment by CO_2 inhalation. The dosage of buprenorphine in serum was measured using the method used in rabbits for the pharmacokinetic study (SI1). Rat paws



were recovered after sacrifice and frozen in nitrogen for immunochemistry.

Statistical analysis

Statistical analyses were performed on StatView SAS 2000 (SAS institute, Cary, NC). For comparison of two groups, non-parametric Mann–Whitney (MW) test was used. The Kruskal–Wallis (KW) test was used to compare three or more independent groups. Significance was set at $p < 0.05$.

Results

Degradable microspheres properties

Morphologically, PEG-MS were similar regardless of their composition (Fig. 1). They were spherical with smooth surfaces, showed no signs of aggregation, and were free of structural defects such as cracks, fused (“Siamese”) microspheres, or inclusions. The mean diameter of PEG-MS was 87 μm , PEG-MS6 had a significantly smaller diameter compared to the other 3 groups (Table S1). The amount of polymer material per 1 mL of wet PEG-MS was 207 mg mL^{-1} (average value for the 4 groups) and it was independent of the composition of the microspheres.

After e-beam treatment (25 kGy), PEG-MS2 were degraded after 2 days in PBS, while PEG-MS6, PEG-MS12 and PEG-MS50 were degraded after 6, 12 and 50 days, respectively (Fig. 2).

The PEG-MS underwent gradual hydrolysis over time, releasing PEGylated degradation products, regardless of their composition. At the end of degradation, no microspheres were visible in PBS. No enzymes were required for degradation of PEG-MS, indicating that degradation occurred *via* a hydrolytic mechanism.²³ The composition of the degradable crosslinker influenced the rate of the PEG-MS degradation; specifically, increasing the caprolactone content relative to lactide resulted in a slower degradation rate (Table S1).

Buprenorphine loading

Low loading levels of buprenorphine (target loading of 1 and 4 mg mL^{-1}) were chosen to minimize systemic passage in an attempt to target peripheral opioid receptors with a systemic exposition as low as possible. In contrast to traditional long acting injectables formulated with poly(lactic-co-glycolic acid)-based microspheres,³⁹ in our approach, buprenorphine loading was performed post-manufacture of the microspheres. It was accomplished through a straightforward process utilizing a purely aqueous solution of the buprenorphine hydrochloride without the addition of any organic solvents.

This method of buprenorphine loading onto the degradable microspheres after their synthesis resulted in a loading efficiency ranging from 75% to 88% for the different loading targets and the different microsphere compositions (Table 2). For loading objectives of 1 mg mL^{-1} and 4 mg mL^{-1} , loading values of 0.8 mg mL^{-1} and 3 mg mL^{-1} were obtained, corresponding to a drug load by weight of 0.3% and 1.4% w/w.

In vitro delivery of buprenorphine according to the microspheres degradation time

The release profiles of buprenorphine from the different PEG-MS after sterilization varied according to their respective degradation time (Fig. 3).

Buprenorphine release closely paralleled the degradation of the microspheres, *i.e.* formulations designed to degrade in 2, 6, and 12 days (PEG-MS2, PEG-MS6, and PEG-MS12, respectively) released the drug over corresponding durations. In the case of the slowest-degrading formulation, PEG-MS50, buprenorphine release plateaued after 30 days while complete degradation of the microsphere occurred after 50 days (Fig. 3B). Overall, the PEG-MS platform enabled sustained buprenorphine release at various rates ranging from 2 days to 30 days as the microspheres degraded without a burst effect. Approximately 90% of the loaded buprenorphine was eluted from the microspheres

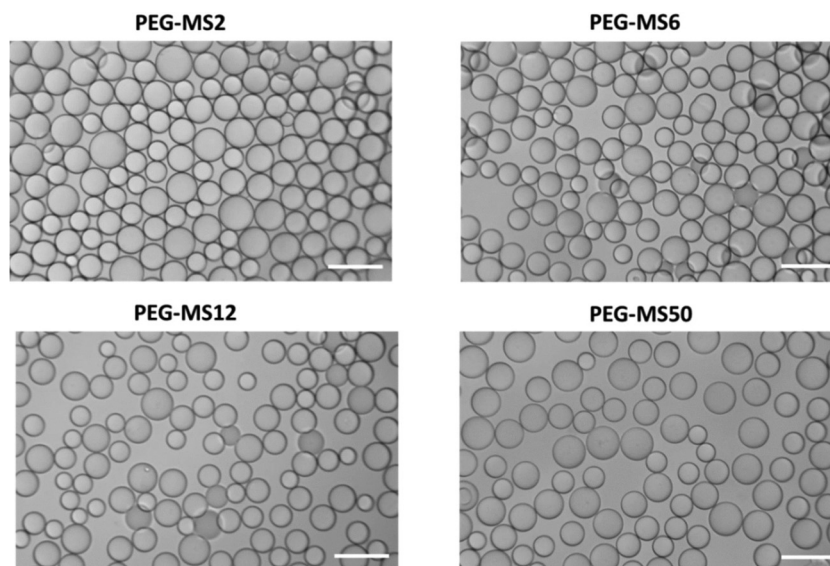


Fig. 1 Aspect of PEG-MS produced by suspension polymerization after sieving (50–100 μm) used for buprenorphine sustained delivery. Bar = 200 μm .



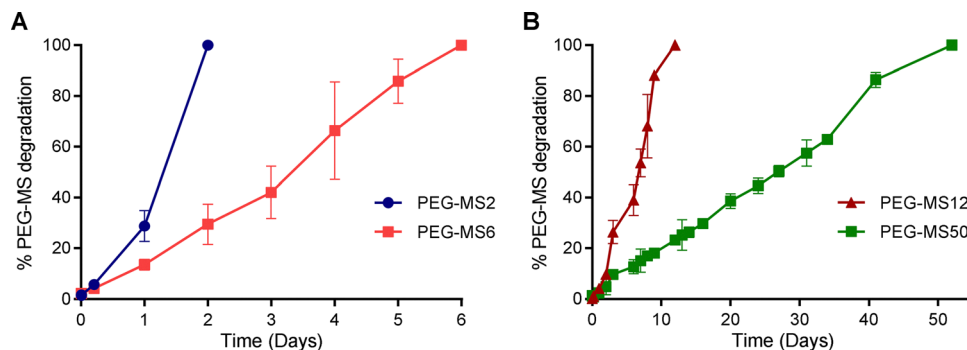


Fig. 2 *In vitro* degradation rate of sterile PEG-MS. The degradation of rapidly degradable (A) and slowly degradable (B) PEG-MS was determined during buprenorphine release on loaded microspheres using an iodine/barium assay of PEGylated products released into the medium over time. Experiments were done in triplicate (PEG-MS2, PEG-MS6, PEG-MS12) and in duplicate (PEG-MS50).

Table 2 Loading values of buprenorphine on PEG-MS for *in vitro* release and preliminary pharmacokinetic study in rabbit. The homogeneity between PEG-MS groups was estimated by the non-parametric Mann–Whitney (MW) and Kruskal–Wallis (KW) tests

Drug loading target	PEG-MS2	PEG-MS6	PEG-MS12	PEG-MS50	Statistical analysis
1 mg mL ⁻¹	0.86 ± 0.03 (n = 9) (85%) ^a	0.88 ± 0.02 (n = 8) (88%)	0.83 ± 0.03 (n = 10) (82%)	0.79 ± 0.02 (n = 2) (79%)	p = 0.0160
4 mg mL ⁻¹	ND	ND	3.03 ± 0.011 (n = 4) (75%)	3.11 ± 0.16 (n = 5) (77%)	p = 0.0731

^a Loading efficiency.

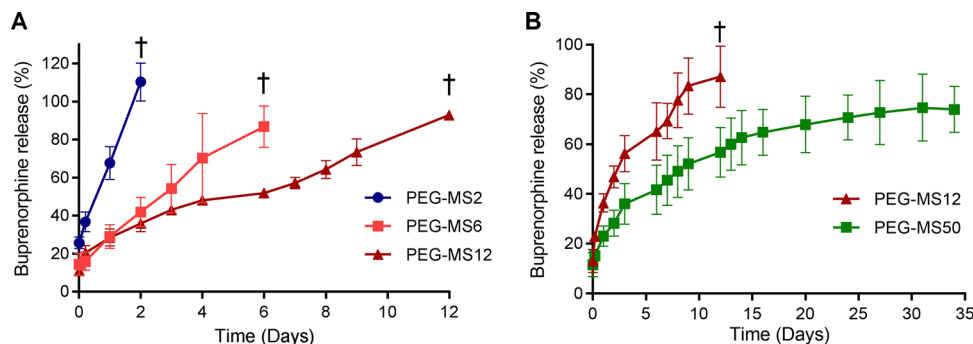


Fig. 3 Buprenorphine release in PBS from degradable PEG-MS loaded at 0.8 mg mL⁻¹ (A) or 3 mg mL⁻¹ (B). Buprenorphine content in medium was determined by fluorimetry (λ_{ex} 280 nm, λ_{em} 354 nm) for PEG-MS2 (n = 3), PEG-MS6 (n = 3), PEG-MS12 at 0.8 mg mL⁻¹ (n = 7), PEG-MS12 (n = 2) and PEG-MS50 (n = 2) at 3 mg mL⁻¹. † PEG-MS degradation time.

that degraded during the release study. For PEG-MS50, it is possible that some of the buprenorphine may have remained bound to the microspheres during the degradation process, which would explain the plateau. Ending buprenorphine elution most often coincided with complete microsphere degradation.

Effect of PEG-MS carriers on buprenorphine concentration in rabbit serum

Prior to testing in a rat model of post-operative pain, a pharmacokinetic study was conducted in rabbits to identify a PEG-MS formulation capable of releasing buprenorphine for at least 3 days after a single subcutaneous administration. All 5 rabbits included in this study remained healthy throughout the study, except for the animal n° 2 injected with PEG-MS2 which somnolent during the first 3 h after administration before

returning to normal behavior. Buprenorphine serum concentrations varied between treatment groups, in particular with regard to C_{max} and duration (Fig. 4). The pharmacokinetic parameters of each formulation are presented in Table 3.

Following subcutaneous administration of Bupaq® (120 µg; 30 µg kg⁻¹/12 h), buprenorphine was detectable in rabbit serum from 15 min to 5 h post-injection, reaching a peak concentration (C_{max}) of 0.59 ng mL⁻¹ at 30 min (Fig. 4A). In contrast, PEG-MS2 resulted in a delayed C_{max} of 1.48 ng mL⁻¹ at 5 h, with detectable levels still present at 24 h. Administration of PEG-MS6 led to stable serum buprenorphine concentrations from 15 min to 48 h. The C_{max} of 0.43 ng mL⁻¹ was observed at 3 h, similar in magnitude to Bupaq®, but with an extended duration of drug presence in the serum. With PEG-MS12, buprenorphine was maintained at consistent levels from 15 min up to 4 days post-injection. A delayed C_{max} of 2.29 ng mL⁻¹ was reached at 24 h. The



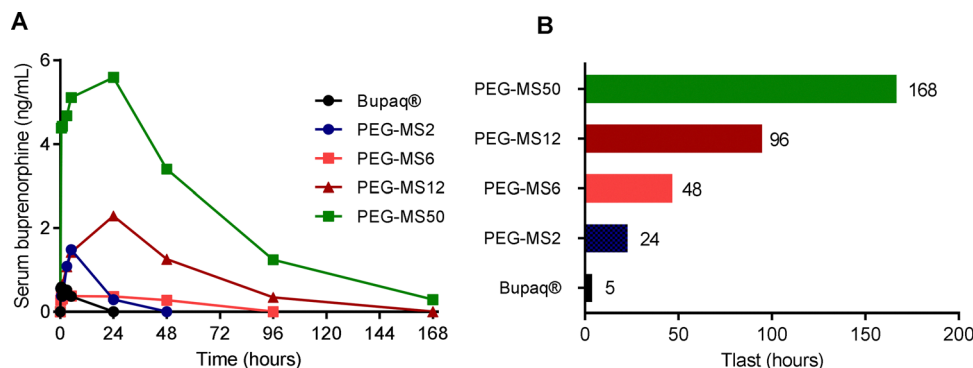


Fig. 4 Serum concentration–time curves showing buprenorphine concentrations in rabbit after a single subcutaneous injection of buprenorphine HCl (Bupaq®) or PEG-MS up to 1 week (A). The time to the last quantifiable serum buprenorphine concentration (T_{last}) corresponded to the last time point where buprenorphine was quantifiable in serum (B). The amounts of buprenorphine and the rationale for dose selection are summarized in Table S2. Pharmacokinetic parameters are summarized in Table 2. All data points are reported. The experiments were carried out on male rabbits.

Table 3 Buprenorphine pharmacokinetic parameters of rabbit after a single subcutaneous injection of PEG-MS loaded with buprenorphine

Animals	Products	Amount of buprenorphine administered (μg)	C_{max} (ng mL^{-1})	T_{max} (h)	$\text{AUC}_{0-T_{\text{last}}}$ ($\text{ng} \times \text{h mL}^{-1}$)	$T_{1/2}$ (h)
1	Bupaq®	120	0.59	0.5	5.6	9.9
2	PEG-MS2	511	1.48	5	24.6	17.9
3	PEG-MS6	1458	0.43	3	22.7	10.5
4	PEG-MS12	2550	2.29	24	132.7	29.9
5	PEG-MS50	6750	5.59	24	399	48.8

PEG-MS50 formulation provided the longest duration of release, with buprenorphine detectable from 15 min to 7 days. Peak concentration reached 5.59 ng mL^{-1} at 24 h, with levels gradually declining to 0.13 ng mL^{-1} by day 7.

$T_{1/2}$ was longer for all PEG-MS formulations compared to injectable Bupaq®. Additionally, $\text{AUC}_{0-T_{\text{last}}}$ increased with both the amount of buprenorphine implanted and the degradation time of PEG-MS (Table 3). The mean time of the last quantifiable serum buprenorphine concentration (T_{last}) also increased with the degradation time of the microspheres (Fig. 4B). These results support the sustained release capacity of PEG-MS formulations, with buprenorphine release closely linked to the degradation profile of each microsphere type.

This study was limited by a small and homogeneous sample population, however, this number was sufficient to show that PEG-MS effectively prolonged buprenorphine release over free buprenorphine in an animal model, confirming *in vitro* observations (Fig. 3). The use of additional animals was therefore not necessary and will go against the Russell and Burch's 3R principles: reduction, refinement, and replacement. For the tactile allodynia study, experimental groups of 10 rats were formed as well as groups of 3 rats for the associated pharmacokinetic study.

Evaluation of the biocompatibility of blank PEG-MS

For the anti-allodynic study in rat, buprenorphine elution from PEG-MS2 and PEG-MS6 were too rapid to cover the post-operative period. As drug release durations from PEG-MS12 and PEG-MS50 were comparable (Fig. 4), PEG-MS12, which degraded in 12 days, was selected for local buprenorphine

administration, in line with the objective of rapid vector clearance following drug release. Prior to *in vivo* efficacy testing, PEG-MS12 biocompatibility was evaluated in rabbits through the administration of the microspheres in 3 tissues: the dermis (tissue of reference for PEG-MS biocompatibility study²³), the muscle at saddle level, and subconjunctival space near the cornea, a tissue rich in functional mu opioid receptors which could be targeted by agonists to reduce ocular pain.¹⁵

Microscopically, PEG-MS12 appeared as ovoid imprints ($\sim 70 \mu\text{m}$ in diameter), either dispersed or in clusters (Fig. 5). Histological analysis on day 2 revealed polymeric material (visible as a purple substance, annotated with a star) inhomogeneously distributed in the tissue indentations, with vacuoles and voids in all tissues. Although the microsphere contours were not regular, no signs of fragmentation or cellular infiltration were observed.

At day 2, PEG-MS12 was detected in all tissues (Table 4), and persisted in at least half of the samples at day 7. After 14 days, no microspheres were detectable in any of the tissues, which was in agreement with the degradation time determined *in vitro* in PBS (Fig. 2). This convergence supports that microsphere degradation in tissues occurred through the hydrolysis of the ester bonds of the crosslinker. The decreasing surface area of microspheres over time confirmed progressive degradation (Fig. 6A), with a notably faster reduction in muscle tissue—dropping from 9.6 mm^2 on day 2 to 0.18 mm^2 by day 7—indicating slightly accelerated degradation at this site (Fig. 6B). Overall, implantation site had minimal impact on degradation kinetics.

On the histology slides ($n = 36$), few cells were visible in the center of the implants or around them in the surrounding



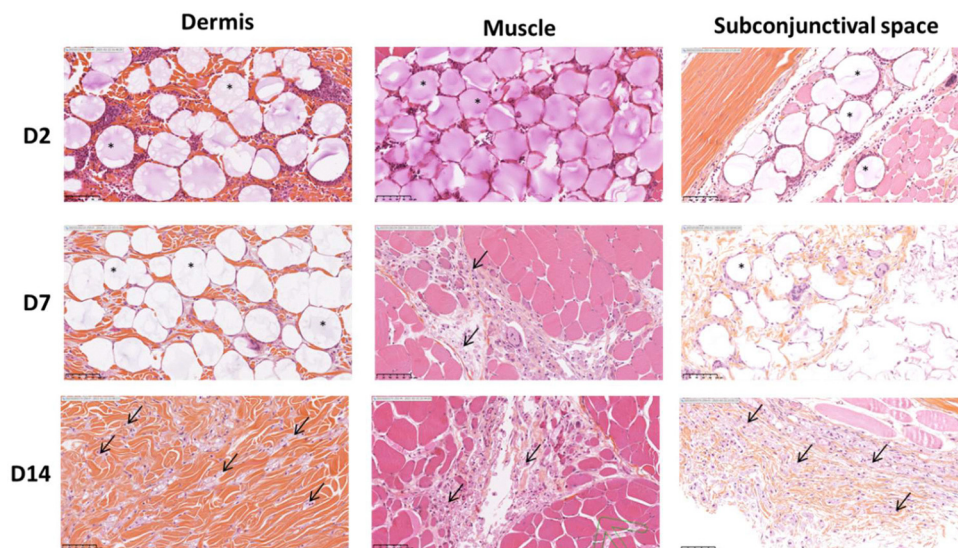


Fig. 5 Histology images of PEG-MS12 at 3 time points in the dermis, muscle and subconjunctival space. PEG-MS12 (100 μ L) were administered in male rabbit ($n = 12$) in the 3 tissues under anesthesia. HES stained sections were digitized. Star (PEG-MS12), arrow (foamy macrophages).

Table 4 Number of samples with PEG-MS12 detected at histopathology for each implantation site and each time point. PEG-MS12 was administered in 4 rabbits for each implantation site

	Day 2	Day 7	Day 14
Dermis	4/4	4/4	0/4
Muscle	4/4	2/4	0/4
Subconjunctival space	3/4	3/4	0/4

tissue, indicating a weak foreign body inflammatory reaction (Fig. 5). No evidence of cell necrosis was observed in any of the three tissues across all time points, confirming the absence of toxic leachables or degradation products and supporting the biocompatibility of the cross-linked PEG-based microspheres.

The thickness of the inflammatory reaction around PEG-MS12 remained limited, increasing slightly from a mean of 14 μ m on day 2 to 27 μ m on day 7, with a maximum of 44 μ m recorded in muscle tissue (Fig. 6C). This thickness then decreased at day 14. Globally, inflammatory response was comparable across tissues, with only a slight transient increase in muscle at day 7.

The type of inflammatory cells associated with PEG-MS12 was determined in skin samples only, as the percentage of neutrophils, eosinophils, lymphocytes, macrophages and giant cells present in 'hotspots' of inflammation. Inflammatory reaction was almost exclusively composed of macrophages and giant cells at all time points while a few neutrophils, eosinophils and lymphocytes were seen at earlier time points and never detected at later time points (Fig. 6D). Macrophages were predominant over giant cells at days 2 and 7. These two cell types showed an increase between the two time points. On day 14, the number of giant cells decreased and foamy macrophages were observed in the dermis between the collagen bundles (Fig. 6D). The purple material observed in their

cytoplasm suggested the presence of phagocytosed polymer indicating that macrophages were cleaning up the tissue.

Anti-allodynic activity of buprenorphine loaded on PEG-MS12 in the Brennan's model in the rat

To evaluate analgesic efficacy, three buprenorphine dosing formulations were prepared for intraplantar injection: blank (drug-free PEG-MS), BU1 (240 μ g buprenorphine; PEG-MS12 at 4.8 mg mL⁻¹), and BU2 (40 μ g buprenorphine; PEG-MS12 at 0.8 mg mL⁻¹). The high dose was chosen to match the reference dose commonly used in commercial sustained-release analgesics for rodents (1.2 mg kg⁻¹).^{35–39}

First of all, evidence of peripheral mu receptors in rat hindpaw was observed on unoperated rat hindpaws, where mu opioid receptor immunoreactivity appeared in nervous structures (Fig. 7).

Labelling was also visible in the epidermis, mainly in the basal cell layers of the keratinocytes and in some endothelial cells. Presence of nerves in paw sections expressing mu receptors indicated that it would be possible to target these receptors using buprenorphine eluted from degradable microspheres to reduce pain induced locally by surgery. However, 3 days after the surgical wound infiltration in the plantar aspect of the foot with a suspension of microspheres, histology failed to show any proximity between the microspheres and the nerve fibres positively labelled with the antibody, suggesting a low density of nerves in the operative wounds.

On days 1, 2, and 3 following surgery and PEG-MS12 infiltration, paw withdrawal thresholds were assessed using the Von Frey test (Fig. 8).

The surgical incision of the plantar aspect of the left hindpaw induced a significant decrease in the paw withdrawal thresholds one-day post-surgery, compared to the control unoperated paw (35 g vs. 59 g, -40%, $p < 0.001$). In the control



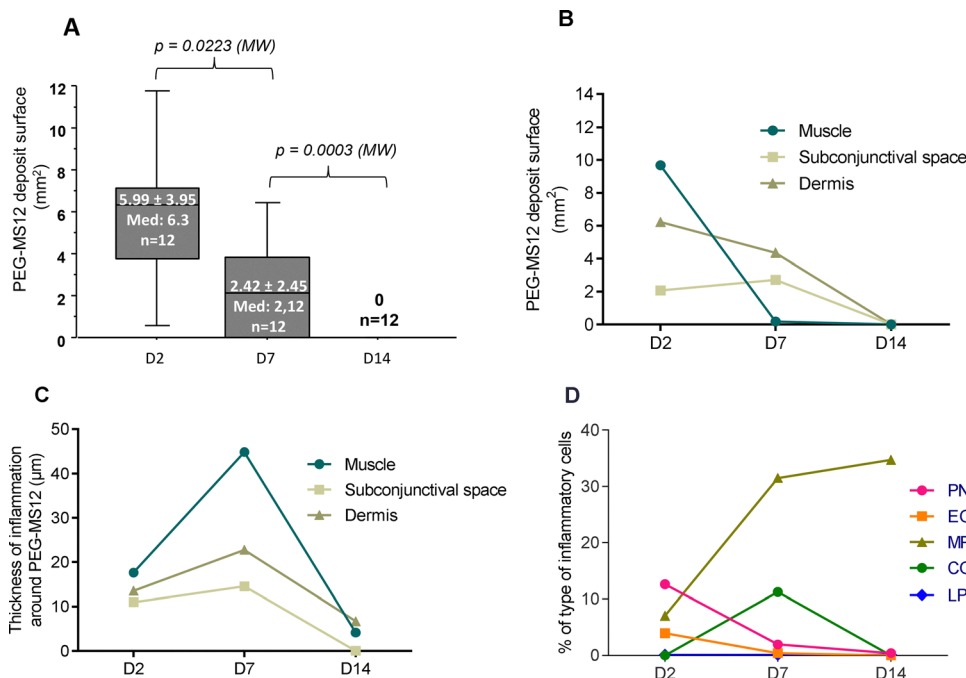


Fig. 6 Quantification of PEG-MS12 degradation at 3 time points in rabbit tissues (A) and (B) and assessment of the inflammatory foreign body reaction observed during microspheres degradation (C) and (D). Evolution of the surface of the implants of PEG-MS12 in all tissue (A) or in each tissue (B). Thickness of inflammation in contact with PEG-MS12 in each tissue (C), evolution of inflammatory cells during PEG-MS12 fate in dermis (D). PN: polymorphonuclear neutrophils, EO: eosinophils, MP: macrophages, CG: giant cells, LP: lymphocytes. The experiments were carried out on male rabbits.

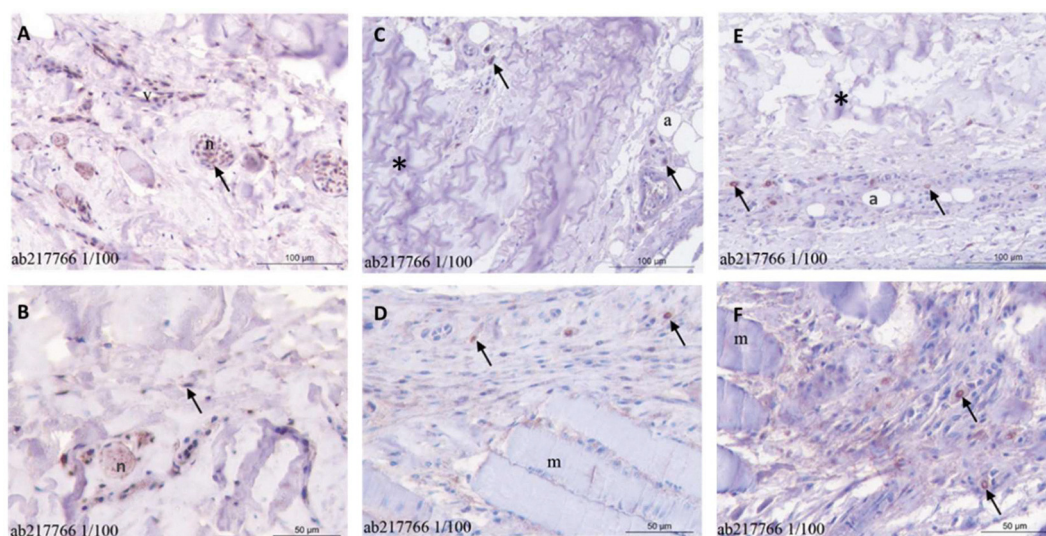


Fig. 7 Detection of mu opioid receptors on rat hindpaws. Unoperated paws (A) and (B) and paws 3 days after plantar incision and intraplantar injection of blank PEG-MS12 (C) and (D) and buprenorphine-loaded PEG-MS12 (240 μg buprenorphine/paw – BU1) (E) and (F). v: vessel, n: nerve, a: adipocyte, m: muscle, arrow: positive cells, star: polymer as filamentous network of bluish color. The negative control of mu opioid receptors labelling is shown in Fig. S2. The experiments were carried out on male rats.

group treated with drug-free PEG-MS (blank), injured paws continued to exhibit significantly lower withdrawal thresholds than the unoperated paws at both day 2 (41 g vs. 52 g, -21% , $p = 0.0011$) and day 3 (42 g vs. 48 g, -12.5% , $p = 0.0194$). Reduction in the withdrawal threshold of the injured paws at day 3 suggested a self-healing process.

The analgesic effect produced by wound infiltration with PEG-MS12 loaded with buprenorphine was determined by comparison with operated hindpaws infiltrated with the drug-free PEG-MS12 in a separate experimental group. Administration of PEG-MS12 loaded with the high dose of buprenorphine (BU1: 240 μg per paw) immediately after surgery significantly

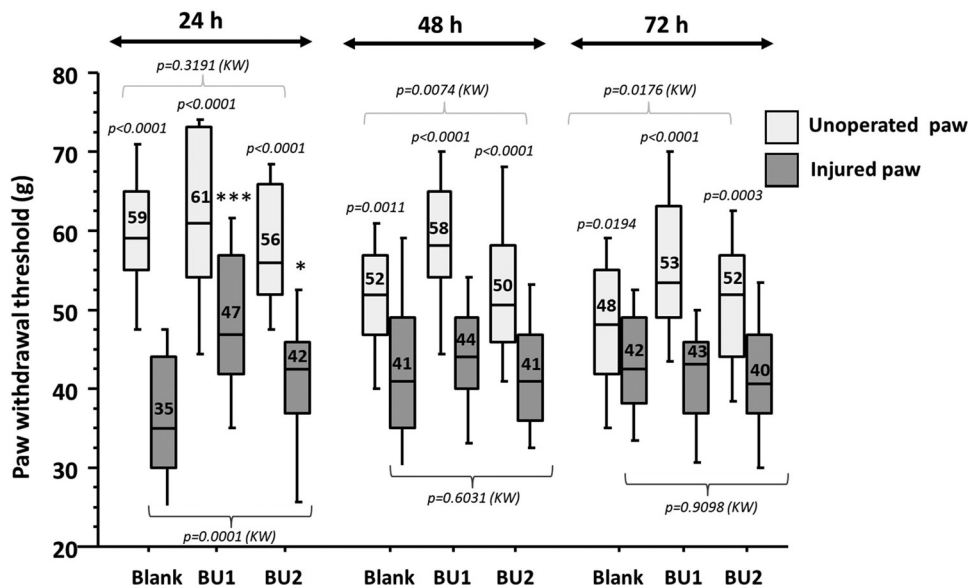


Fig. 8 Effect on tactile allodynia of PEG-MS12 loaded with buprenorphine intraplantarly injected in the incisional pain model in rat. The tactile allodynia produced by the incision was quantified using the electronic Von Frey test. Paw withdrawal threshold was measured in 10 male rats per group starting 1 day after surgery and PEG-MS12 injection. The paw withdrawal threshold values were expressed as medians. Comparison of the paw withdrawal threshold values between the unoperated paws and injured paws was done using the Mann–Whitney (MW) non-parametric test. The effect of locally injected buprenorphine loaded on PEG-MS12 in the injured paw (BU1: 240 μ g buprenorphine/paw, BU2: 40 μ g buprenorphine/paw) was compared to the vehicle-treated paw (blank PEG-MS) using the MW non-parametric test (* $p = 0.0466$, *** $p < 0.0001$). The Kruskal–Wallis (KW) test was used to compare the 3 experimental groups (blank, BU1 and BU2) at each time for the non-operated paws (values at the top of the graph) and for the paws operated and infiltrated by microspheres with or without buprenorphine (values at the bottom of the graph).

improved withdrawal thresholds at day 1 compared to the drug-free PEG-MS group (47 g vs. 35 g; +34%, $p < 0.0001$). A similar but less pronounced effect was observed with the low-dose buprenorphine formulation (BU2: 40 μ g per paw), which also resulted in a significantly higher threshold than the blank group (42 g vs. 35 g; +20%, $p = 0.0466$). However, by day 2 ($p = 0.6031$, KW) and day 3 ($p = 0.9098$, KW), no significant differences in withdrawal thresholds were observed between the blank, BU1, and BU2 groups.

As a tissue assay of buprenorphine was not performed in hindpaws, a serum assay was conducted to monitor systemic drug concentrations. The aim was to facilitate the interpretation of allodynia measurements in relation to serum concentrations of buprenorphine, and more specifically to determine whether the pain relief observed at 24 h was explained by a local or systemic effect. The rat blood concentration of buprenorphine following the intraplantar injection of PEG-MS12 was assessed (Fig. 9).

The circulating concentrations of buprenorphine decreased over time. For the highest dose (240 μ g per paw; 4.8 mg mL⁻¹), serum concentrations remained above the therapeutic threshold in rodents (1 ng mL⁻¹), with level measured at 2.21 ng mL⁻¹ at 24 h and 1.24 ng mL⁻¹ at 48 h. For the low dose (40 μ g per paw; 0.8 mg mL⁻¹), the circulating concentration of buprenorphine was lower than the therapeutic threshold at 24 h and 48 h. In each experimental group, buprenorphine was absent from serum samples at 72 h.

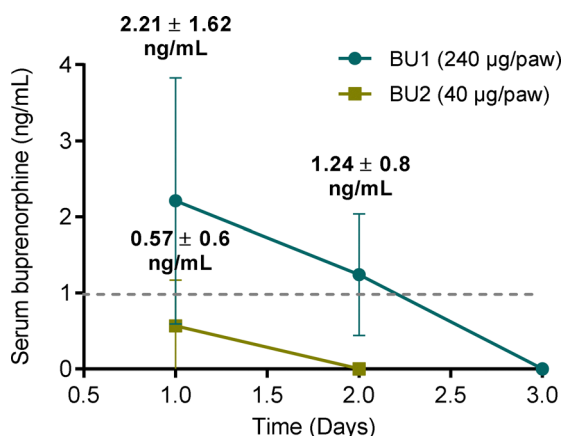


Fig. 9 Serum concentration of buprenorphine after the intraplantar administration at high (BU1) and low dose (BU2) of PEG-MS12 loaded with buprenorphine. The dosing was performed on 3 male rats at each time point and at each dose level during 3 days.

Discussion

The identification of functional opioid receptors in peripheral tissues has opened new avenues for managing postoperative pain while minimizing central opioid side effects.^{19,20} This study aimed to investigate the potential of a local, sustained-release strategy for postoperative pain management using low doses of buprenorphine delivered *via* a degradable drug delivery system (DDS). Specifically, we examined whether PEG-based



hydrophilic microspheres (PEG-MS) could provide prolonged peripheral analgesia by gradually releasing buprenorphine at the site of surgical injury, thereby activating peripheral opioid receptors. The primary objective was to demonstrate that PEG-MS can serve as an effective DDS for the sustained release of buprenorphine. A secondary goal was to test the hypothesis that locally released buprenorphine can activate peripheral opioid receptors to achieve postoperative analgesia in a rat model of incisional pain.

Buprenorphine loading onto PEG-MS and its sustained release

The sustained-release strategy for buprenorphine developed in this study draws inspiration from chemoembolization, where drugs in aqueous solution like doxorubicin or irinotecan are loaded onto pre-calibrated microspheres *via* ionic interactions before being delivered intra-arterially through a micro-catheter.^{28,29} The degradable PEG-MS, originally developed for embolization^{23,40,41} and chemoembolization^{24,25} were adapted here for local administration.

Buprenorphine in water was efficiently loaded on different PEG-MS with four degradation times. Given buprenorphine's lipophilic nature ($\log P = 4.98$), loading probably occurred *via* hydrophobic interactions with the caprolactone and lactide moieties present in the degradable crosslinkers. This approach aligns with established strategies for incorporating lipophilic drugs into hydrogels through hydrophobic domains.^{42,43} The amphiphilic nature of PEG-MS not only facilitates effective loading of hydrophobic drugs like buprenorphine but also ensures a better biocompatibility and promotes rapid fate in tissues.

Buprenorphine release was strongly correlated with PEG-MS degradation time, confirming its interaction with the cross-linked PEG polymer. Following subcutaneous injection in rabbits, the four PEG-MS formulations produced a rapid serum peak, indicating immediate bioavailability for early analgesic effect. Subsequently, buprenorphine was gradually released as the PEG-MS degraded, supporting a prolonged analgesic action. However, the small number of rabbits used in the pharmacokinetic study limited the possibility of statistical analysis. Overall, the administration of buprenorphine loaded PEG-MS ($n = 4$) showed that the microspheres delayed the serum passage of buprenorphine. Collectively the material effect was shown to be consistent with microsphere degradation times. The release profiles paralleled the degradation kinetics of each formulation, in contrast to delivery systems based on poly(lactic-co-glycolic acid), lactide, caprolactone, or their copolymers, where drug release occurs over a few days despite matrix degradation taking months or years.^{44,45} Due to the rapid degradation of PEG-MS, the risk of a long-term inflammatory reaction around the implant after buprenorphine delivery is abolished, which is an advantage for treatment tolerance.

Trial of peripheral analgesia in the rat's brenann model

Following intraplantar injection of buprenorphine-loaded PEG-MS, the aim was to achieve sustained targeting of opioid

receptors through gradual buprenorphine release, overcoming tissue clearance to maintain effective local concentrations over several days. However, this objective was only partially achieved. PEG-MS with lower dose of buprenorphine (40 μg per paw) resulted in minimal systemic exposure but produced limited efficacy on tactile allodynia at the limit of significance. In contrast, a single intraplantar administration of PEG-MS loaded with the high dose of buprenorphine (240 μg per paw) induced a significant anti-allodynic effect as evidenced by an increase in the paw withdrawal threshold (+34%) at day 1 compared to the vehicle-treated group. However, serum concentrations at this time point were above the therapeutic threshold (1 ng ml^{-1}), indicating that the analgesic effect was likely mediated by systemic—rather than local—opioid receptor activation. Furthermore, reduction in allodynia at 48 h was not observed, probably because the concentration of buprenorphine was near the threshold of efficacy in rodents. In the Brennan model, the high local dose of 240 μg of buprenorphine was equivalent to a dose of 1.2 mg kg^{-1} when expressed in terms of animal body weight. This dose was similar to buprenorphine sustained-release formulations marketed for analgesia in rats, which provide analgesia for 48–72 h in several pain models after a single subcutaneous injection.^{36–38} The results obtained with PEG-MS were close to those obtained with PLGA microspheres in development, which provide *in vivo* release of buprenorphine for 3 days after single subcutaneous administration depending on microsphere diameter and polymer molecular weight, with 30% burst and plasma levels above 1 ng ml^{-1} for 24 h in mice at 1.2 mg kg^{-1} .³⁹ Despite the absence of clear evidence for local receptor engagement, PEG-MS12 enabled effective postoperative analgesia during 24 h at a clinically relevant dose, most likely through systemic drug release.

Targeting of mu opioid receptor

The main limitation of the intraplantar implantation of PEG-MS after surgery was the potential loss of PEG-MS from the surgical site. To mitigate this risk, an additional (third) suture bridge was performed, instead of the two described in the original method.³² Then, using stained microspheres, it was found that under the conditions of the study, the PEG-MS did not get released when the rats walked. Despite this, upon recovery from anesthesia, the return to normal mobility and frequent pressure exerted on the operated paw during ambulation may have induced microsphere leakage, potentially reducing the effective dose of buprenorphine. This potential loss of material could have impacted the observed analgesic efficacy. To improve reliability and ensure consistent drug delivery, further studies should be conducted with PEG-MS injected subcutaneously at a dose of 1.2 mg kg^{-1} , aligning with protocols used in previous evaluations of sustained-release buprenorphine formulations in rodent pain models.^{36–39} Once implanted subcutaneously, the microspheres cannot be released by animal movement. Another possible explanation is the possible loss of buprenorphine through wound exudate following suturing. Interstitial fluid containing buprenorphine



may have escaped through the wound under mechanical pressure during walking. An alternative hypothesis to account for the absence of local anti-allodynic activity is the paucity of mu opioid receptors in the vicinity of degradable PEG-MS, whereas one might have expected overexpression of mu opioid receptors after surgery.⁴⁶

Changes in buprenorphine delivery time

This study observed a rapid decline in the release time of buprenorphine since PEG-MS12 transitioned from 12 days in PBS to four days in rabbits and 24 h in rats, providing 24 h of pain relief. The accelerated release of buprenorphine after subcutaneous implantation in rabbits was consistent with previous reports showing that the *in vivo* absorption curves of long-acting injectable formulations could be different from the *in vitro* release profiles.⁴⁷ These differences can be explained by the *in vitro* release methods, such as the apparatus, release media, vessel dimensions, temperature, and agitation speed. The *in vitro* release method for buprenorphine-loaded PEG-MS needs improvement to achieve a better *in vitro-in vivo* correlations. On the other hand, the acceleration of buprenorphine absorption between subcutaneous injections in rabbits and intraplantar injections in rats could be explained by a different lymphatic drainage between the two injection sites. It is acknowledged that lymph production is increased by mechanical stimuli such as arterial pulsation, vibration, massage and joint movement.⁴⁸ It is therefore conceivable that lymph drainage in the hindpaws, on which the rats lean when walking, was greater than in the rabbit's subcutaneous tissue, thereby stimulating the passage of buprenorphine into the blood circulation. In the skin, the hydrostatic pressure of tissue fluid is negative, and the pressure in the initial lymphatics to be positive, some driving force is necessary for lymph to be produced against this pressure gradient.^{48,49} Another possible explanation for the rapid decline in buprenorphine concentration in rat serum was a faster elimination in rats than in rabbits, where detectable levels persist for up to four days after subcutaneous injection of PEG-MS. Clearance measures done in rodents and rabbits after intravenous injection of buprenorphine support this hypothesis, since clearance values of 2.8 and 4.1 l h⁻¹ kg⁻¹ were reported for rats and 1.8 l h⁻¹ kg⁻¹ for rabbit.⁵⁰

PEG-MS a biocompatible degradable DDS

Ideally, a DDS would be resorbed after drug delivery with little tissue reaction, which is not the case with the lactide and caprolactone-based injectable gel for buprenorphine (buprenorphine ER-LAB formulation) which degrades over years.^{44,45} The degradation rate of PEG-MS could be tuned by varying the caprolactone content in the degradable crosslinker. Incorporation of caprolactone extended the degradation time from 2 days (crosslinker without Cl) to up to 2 months with the more hydrophobic crosslinker composition (PEG₁₃-LA₄-co-Cl₅). The slowing down of degradation by caprolactone was described with different copolymers composed of poly(L-lactide) and poly(ε-caprolactone).^{51,52} The hydrogel composition of

PEG-MS contributes to the low intensity of the foreign body inflammatory response observed in various rabbit tissues during microspheres degradation. This PEG hydrogel formulated in microspheres contains a small amount of polyesters and PEG material (approximately 20% of the mass), with the majority of the mass being water. Mild and transient inflammation has previously been observed in the rabbit dermis following degradation of PEG-MS within 24–48 h²³ and in the sheep shoulder joint cavity with slower-degrading PEG-MS,⁵³ confirming the excellent local biocompatibility of cross-linked PEG hydrogels. In terms of overall safety, PEG-MS for buprenorphine delivery combines several advantages: absence of organic solvent, low amount of polymer, rapid degradation with mild inflammatory reaction, and use of buprenorphine hydrochloride rather than buprenorphine base as the active ingredient, which is more toxic than the hydrochloride salt.⁶

Other strategies for achieving peripheral analgesia with opioids

In order to limit the systemic diffusion of buprenorphine into the circulation by oral or intravenous treatments, local injection of opioid solutions into wounds has been investigated.¹⁰ The therapeutic effect is short-lived (≈6 h) and depends on the inflammation of the treated tissues. In this study, local implantation of a buprenorphine DDS resulted in plasma absorption of a therapeutic dose, confirming that local treatments pose a risk of systemic exposure. This has been well demonstrated for local anesthetics injected along nerve pathways, where systemic absorption is strictly controlled to prevent toxic plasma levels.⁵⁴ With the aim of eliminating the undesirable side effects of opioids by selectively activating opioid receptors outside the central nervous system, several experimental approaches are being developed. One of these is the development of nanoparticles, such as nanocarriers of morphine²¹ or neuropeptide Leu-enkephalin⁵⁵ or liposomes conjugated to the intracellular adhesion molecule I (ICAM-1) antibody loaded with the mu receptor antagonist iopermaide⁵⁶ for peripheral delivery into inflamed tissues for pain control based on the enhanced permeability and retention (EPR) effect. Opioid derivatives with low blood brain barrier penetration have been developed, such as asimadoline (peripheral K receptors), which has been tested in clinical trials in patients with irritable bowel syndrome (NCT00454688) or after colectomy (NCT00443040). The acidity of fluids in injured and inflamed tissues (pH 5–7) vs. 7.4 in non-inflamed tissues has been taken into consideration to develop derivatives that are only ionized in an acidic environment in order to activate opioid receptors in tissues where the micro-environment is acidic. Such a compound called NFEPP (pK_a 6.8), which is only active in acidic tissues caused by injury/inflammation, was obtained by fluorination of fentanyl (pK_a 8.43). NFEPP binds to the mu opioid receptor and activates it only at acidic pH, producing analgesia in different animal pain models.^{19,57} To get an opioid based analgesia without side effects the answers are manifold, combining on the one hand the design of new prototypes of opioid receptor ligands and on the other the development of vectors for their appropriate administration.



Conclusion

The initial objective of achieving peripheral analgesia by targeting mu receptors after infiltrating a buprenorphine DDS into the plantar wound of the rat's Brennan model was inconclusive due to the brief duration of analgesia (24 h) and the systemic passage of buprenorphine released from degradable microspheres. The reasons for this failure may be multiple, including the low density of mu opioid receptors in the surgical wound, the loss of part of the microspheres or buprenorphine-containing exudate from the wound, or the high lymphatic drainage stimulated by the movement of rats on their operated hindpaws. However, compared to existing buprenorphine DDS, the solvent-free PEG-MS due to its rapid degradation, absence of organic solvent and biocompatibility make then a promising degradable platform for buprenorphine delivery for post-operative pain relief in pets and laboratory animals after subcutaneous administration like the two prolonged-release buprenorphine formulations on the market in United States.^{36–39} Further studies in incisional models after subcutaneous injection in rats⁵⁸ and pigs^{59,60} could confirm the potential shown in this study to alleviate the post-operative pain. The route of administration and the dose of buprenorphine to be loaded onto the PEG-MS must be optimized for the different possible clinical indications.

Author contributions

All authors have contributed substantially to the manuscript: LB & LM conceived the project, AB and ES managed the chemistry work, JN designed the *in vivo* experiments, FP conducted the *in vivo* experiments, MW and SHG interpreted the histology data, LM supervised the study and validated the final version of the manuscript. LB and AB wrote the manuscript. Authors state that this study is not submitted or published elsewhere.

Conflicts of interest

AB, ES, LB are employees of Occlugel. The research reported in this publication was funded by Occlugel company. The authors (LB, AB, ES, LM) are co-inventors of patents on resorbable microspheres co-owned by Occlugel company and Public Institutions (CNRS, AP-HP, Universities of Paris Diderot & Saclay).

Data availability

We confirm that the majority of the data supporting the conclusions of our study are available in the article and its SI. Additional data are available from the corresponding author upon reasonable request. See DOI: <https://doi.org/10.1039/d5tb01312g>

Acknowledgements

The study was funded by Occlugel company.

References

- 1 J. L. Apfelbaum, C. Chen, S. S. Mehta and T. J. Gan, Postoperative Pain Experience: Results from a National Survey Suggest Postoperative Pain Continues to Be Undermanaged, *Anesth. Analg.*, 2003, **97**, 534–540, DOI: [10.1213/01.ANE.0000068822.10113.9E](https://doi.org/10.1213/01.ANE.0000068822.10113.9E).
- 2 G. P. Dobson, Trauma of major surgery: A global problem that is not going away, *Int. J. Surg.*, 2020, **81**, 47–54, DOI: [10.1016/j.ijssu.2020.07.017](https://doi.org/10.1016/j.ijssu.2020.07.017).
- 3 J. Bruce and J. Quinlan, Chronic Post Surgical Pain, *Rev. Pain*, 2011, **5**, 23–29, DOI: [10.1177/204946371100500306](https://doi.org/10.1177/204946371100500306).
- 4 K. Lutfy and A. Cowan, Buprenorphine: A Unique Drug with Complex Pharmacology, *Curr. Neuropharmacol.*, 2004, **2**, 395–402, DOI: [10.2174/1570159043359477](https://doi.org/10.2174/1570159043359477).
- 5 S. Butler, Buprenorphine—Clinically useful but often misunderstood, *Scand. J. Pain*, 2013, **4**, 148–152, DOI: [10.1016/j.sjpain.2013.05.004](https://doi.org/10.1016/j.sjpain.2013.05.004).
- 6 R. E. Johnson, P. J. Fudala and R. Payne, Buprenorphine: Considerations for Pain Management, *J. Pain Symptom Manage.*, 2005, **29**, 297–326, DOI: [10.1016/j.jpainsymman.2004.07.005](https://doi.org/10.1016/j.jpainsymman.2004.07.005).
- 7 R. B. Raffa, M. Haidery, H. M. Huang, K. Kalladeen, D. E. Lockstein, H. Ono, M. J. Shope, O. A. Sowunmi, J. K. Tran and J. V. Pergolizzi, The clinical analgesic efficacy of buprenorphine, *J. Clin. Pharm. Ther.*, 2014, **39**, 577–583, DOI: [10.1111/jcpt.12196](https://doi.org/10.1111/jcpt.12196).
- 8 L. D. White, A. Hodge, R. Vlok, G. Hurtado, K. Eastern and T. M. Melhuish, Efficacy and adverse effects of buprenorphine in acute pain management: systematic review and meta-analysis of randomised controlled trials, *Br. J. Anaesth.*, 2018, **120**, 668–678, DOI: [10.1016/j.bja.2017.11.086](https://doi.org/10.1016/j.bja.2017.11.086).
- 9 J. Strang, A. Knight, S. Baillie, K. Reed, K. Bogdanowicz and J. Bell, Norbuprenorphine and respiratory depression: Exploratory analyses with new lyophilized buprenorphine and sublingual buprenorphine, *Int. J. Clin. Pharmacol. Ther.*, 2018, **56**, 81–85, DOI: [10.5414/CP203118](https://doi.org/10.5414/CP203118).
- 10 B. N. Nielsen, S. W. Henneberg, K. Schmiegelow, S. M. Friis and J. Rømsing, Peripherally applied opioids for postoperative pain: evidence of an analgesic effect? A systematic review and meta-analysis, *Acta Anaesthesiol. Scand.*, 2015, **59**, 830–845, DOI: [10.1111/aas.12529](https://doi.org/10.1111/aas.12529).
- 11 N. J. W. Russell, H.-G. Schaible and R. F. Schmidt, Opiates inhibit the discharges of fine afferent units from inflamed knee joint of the cat, *Neurosci. Lett.*, 1987, **76**, 107–112, DOI: [10.1016/0304-3940\(87\)90201-1](https://doi.org/10.1016/0304-3940(87)90201-1).
- 12 C. Stein, K. Comisel, E. Haimerl, A. Yassouridis, K. Lehrberger, A. Herz and K. Peter, Analgesic Effect of Intraarticular Morphine after Arthroscopic Knee Surgery, *N. Engl. J. Med.*, 1991, **325**, 1123–1126, DOI: [10.1056/NEJM199110173251602](https://doi.org/10.1056/NEJM199110173251602).
- 13 R. E. Coggeshall, S. Zhou and S. M. Carlton, Opioid receptors on peripheral sensory axons, *Brain Res.*, 1997, **764**, 126–132, DOI: [10.1016/S0006-8993\(97\)00446-0](https://doi.org/10.1016/S0006-8993(97)00446-0).
- 14 J. P. A. M. van Loon, J. C. de Grauw, A. Brunott, E. A. W. S. Weerts and P. R. van Weeren, Upregulation of articular synovial membrane μ -opioid-like receptors in an



- acute equine synovitis model, *Vet. J.*, 2013, **196**, 40–46, DOI: [10.1016/j.tvjl.2012.07.030](https://doi.org/10.1016/j.tvjl.2012.07.030).
- 15 F. Joubert, A. Guerrero-Moreno, D. Fakih, E. Reboussin, C. Gaveriaux-Ruff, M. C. Acosta, J. Gallar, J. A. Sahel, L. Bodineau, C. Baudouin, W. Rostène, S. Mélik-Parsadaniantz and A. Réaux-Le Goazigo, Topical treatment with a mu opioid receptor agonist alleviates corneal allodynia and corneal nerve sensitization in mice, *Biomed. Pharmacother.*, 2020, **132**, 110794, DOI: [10.1016/j.biopha.2020.110794](https://doi.org/10.1016/j.biopha.2020.110794).
 - 16 A. H. S. Hassan, A. Ableitner, C. Stein and A. Herz, Inflammation of the rat paw enhances axonal transport of opioid receptors in the sciatic nerve and increases their density in the inflamed tissue, *Neuroscience*, 1993, **55**, 185–195, DOI: [10.1016/0306-4522\(93\)90465-r](https://doi.org/10.1016/0306-4522(93)90465-r).
 - 17 E. M. Mambretti, K. Kistner, S. Mayer, D. Massotte, B. L. Kieffer, C. Hoffmann, P. W. Reeh, A. Brack, E. Asan and H. L. Rittner, Functional and structural characterization of axonal opioid receptors as targets for analgesia, *Mol. Pain*, 2016, **12**, 174480691662873, DOI: [10.1177/1744806916628734](https://doi.org/10.1177/1744806916628734).
 - 18 P. Holzer, Opioids and opioid receptors in the enteric nervous system: from a problem in opioid analgesia to a possible new prokinetic therapy in humans, *Neurosci. Lett.*, 2004, **361**, 192–195, DOI: [10.1016/j.neulet.2003.12.004](https://doi.org/10.1016/j.neulet.2003.12.004).
 - 19 H. Machelska and M. Ö. Celik, Advances in Achieving Opioid Analgesia Without Side Effects, *Front. Pharmacol.*, 2018, **9**, 1388, DOI: [10.3389/fphar.2018.01388](https://doi.org/10.3389/fphar.2018.01388).
 - 20 M. Spetea, Opioid Receptors and Their Ligands in the Musculoskeletal System and Relevance for Pain Control, *Curr. Pharm. Des.*, 2014, **19**, 7382–7390, DOI: [10.2174/13816128113199990363](https://doi.org/10.2174/13816128113199990363).
 - 21 S. González-Rodríguez, M. A. Quadir, S. Gupta, K. A. Walker, X. Zhang, V. Spahn, D. Labuz, A. Rodríguez-Gaztelumendi, M. Schmelz, J. Joseph, M. K. Parr, H. Machelska, R. Haag and C. Stein, Polyglycerol-opioid conjugate produces analgesia devoid of side effects, *eLife*, 2017, **6**, DOI: [10.7554/eLife.27081](https://doi.org/10.7554/eLife.27081).
 - 22 M. Chappuy, B. Trojak, P. Nubukpo, J. Bachellier, P. Bendimerad, G. Brousse and B. Rolland, Prolonged-release buprenorphine formulations: Perspectives for clinical practice, *Therapies*, 2020, **75**, 397–406, DOI: [10.1016/j.therap.2020.05.007](https://doi.org/10.1016/j.therap.2020.05.007).
 - 23 S. Louguet, V. Verret, L. Bédouet, E. Servais, F. Pascale, M. Wassef, D. Labarre, A. Laurent and L. Moine, Poly(ethylene glycol) methacrylate hydrolyzable microspheres for transient vascular embolization, *Acta Biomater.*, 2014, **10**, 1194–1205.
 - 24 L. Bédouet, V. Verret, S. Louguet, E. Servais, L. Moine and A. Laurent, Doxorubicin, irinotecan and sunitinib: loading and release with a resorbable embolization microsphere (REM), *J. Vasc. Interventional Radiol.*, 2013, **24**, S48, DOI: [10.1016/j.jvir.2013.01.109](https://doi.org/10.1016/j.jvir.2013.01.109).
 - 25 L. Bédouet, V. Verret, S. Louguet, E. Servais, F. Pascale, A. Beilvert, M. T. Baylatry, D. Labarre, L. Moine and A. Laurent, Anti-angiogenic drug delivery from hydrophilic resorbable embolization microspheres: An *in vitro* study with sunitinib and bevacizumab, *Int. J. Pharm.*, 2015, **484**, 218–227, DOI: [10.1016/j.ijpharm.2015.02.039](https://doi.org/10.1016/j.ijpharm.2015.02.039).
 - 26 L. Magnon, A. Laurent, M. Wassef, L. Bédouet, S. Louguet, V. Verret and E. Servais *Implantable swellable bio-resorbable polymer*, WO 2012/120138 A1, 2012.
 - 27 L. Magnon, A. Laurent, M. Wassef, L. Bédouet, S. Louguet, V. Verret and E. Servais *Implantable bio-resorbable polymer charged with fragiles macromolecules*, WO 2012/120139 A1, 2012.
 - 28 T. de Baere, S. Plotkin, R. Yu, A. Sutter, Y. Wu and G. M. Cruise, An In Vitro Evaluation of Four Types of Drug-Eluting Microspheres Loaded with Doxorubicin, *J. Vasc. Interventional Radiol.*, 2016, **27**, 1425–1431, DOI: [10.1016/j.jvir.2016.05.015](https://doi.org/10.1016/j.jvir.2016.05.015).
 - 29 K. Fuchs, R. Duran, A. Denys, P. E. Bize, G. Borchard and O. Jordan, Drug-eluting embolic microspheres for local drug delivery – State of the art, *J. Controlled Release*, 2017, **262**, 127–138, DOI: [10.1016/j.jconrel.2017.07.016](https://doi.org/10.1016/j.jconrel.2017.07.016).
 - 30 L. Bédouet, L. Moine, E. Servais, A. Beilvert, D. Labarre and A. Laurent, Tunable delivery of niflumic acid from resorbable embolization microspheres for uterine fibroid embolization, *Int. J. Pharm.*, 2016, **511**, 253–261, DOI: [10.1016/j.ijpharm.2016.06.128](https://doi.org/10.1016/j.ijpharm.2016.06.128).
 - 31 X. W. Gong, D. Z. Wei, M. L. He and Y. C. Xiong, Discarded free PEG-based assay for obtaining the modification extent of pegylated proteins, *Talanta*, 2007, **71**, 381–384, DOI: [10.1016/j.talanta.2006.04.010](https://doi.org/10.1016/j.talanta.2006.04.010).
 - 32 T. J. Brennan, E. P. Vandermeulen and G. F. Gebhart, Characterization of a rat model of incisional pain, *Pain*, 1996, **64**, 493–502, DOI: [10.1016/0304-3959\(95\)01441-1](https://doi.org/10.1016/0304-3959(95)01441-1).
 - 33 P. Jirkof, A. Tourvieille, P. Cinelli and M. Arras, Buprenorphine for pain relief in mice: repeated injections vs. sustained-release depot formulation, *Lab. Anim.*, 2015, **49**, 177–187, DOI: [10.1177/0023677214562849](https://doi.org/10.1177/0023677214562849).
 - 34 L. I. Curtin, J. A. Grakowsky, M. Suarez, A. C. Thompson, J. M. DiPirro, L. B. Martin and M. B. Kristal, Evaluation of buprenorphine in a postoperative pain model in rats, *Comp. Med.*, 2009, **59**, 60–71.
 - 35 J. Rudeck, S. Vogl, C. Heinl, M. Steinfath, S. Fritzwanker, A. Kliewer, S. Schulz, G. Schönfelder and B. Bert, Analgesic treatment with buprenorphine should be adapted to the mouse strain, *Pharmacol., Biochem. Behav.*, 2020, **191**, 172877, DOI: [10.1016/j.pbb.2020.172877](https://doi.org/10.1016/j.pbb.2020.172877).
 - 36 P. L. Foley, H. Liang and A. R. Crichlow, Evaluation of a sustained-release formulation of buprenorphine for analgesia in rats, *J. Am. Assoc. Lab. Anim. Sci.*, 2011, **50**, 198–204.
 - 37 H. H. Chum, K. Jampachaisri, G. P. McKeon, D. C. Yeomans, C. Pacharinsak and S. A. Felt, Antinociceptive effects of sustained-release buprenorphine in a model of incisional pain in rats (*Rattus norvegicus*), *J. Am. Assoc. Lab. Anim. Sci.*, 2014, **53**, 193–197.
 - 38 E. D. Alamaw, B. D. Franco, K. Jampachaisri, M. K. Huss and C. Pacharinsak, Extended-release Buprenorphine, an FDA-indexed Analgesic, Attenuates Mechanical Hypersensitivity in Rats (*Rattus norvegicus*), *J. Am. Assoc. Lab. Anim. Sci.*, 2022, **61**, 81–88.



- 39 V. Schreiner, M. Durst, M. Arras, P. Detampel, P. Jirkof and J. Huwyler, Design and in vivo evaluation of a microparticulate depot formulation of buprenorphine for veterinary use, *Sci. Rep.*, 2020, **10**, 17295, DOI: [10.1038/s41598-020-74230-6](https://doi.org/10.1038/s41598-020-74230-6).
- 40 N. Maeda, V. Verret, L. Moine, L. Bédouet, S. Louguet, E. Servais, K. Osuga, N. Tomiyama, M. Wassef and A. Laurent, Targeting and Recanalization after Embolization with Calibrated Resorbable Microspheres versus Hand-cut Gelatin Sponge Particles in a Porcine Kidney Model, *J. Vasc. Interventional Radiol.*, 2013, **24**, 1391–1398, DOI: [10.1016/j.jvir.2013.05.058](https://doi.org/10.1016/j.jvir.2013.05.058).
- 41 V. Verret, J. P. Pelage, M. Wassef, S. Louguet, E. Servais, L. Bédouet, T. Beaulieu, L. Moine and A. Laurent, A Novel Resorbable Embolization Microsphere for Transient Uterine Artery Occlusion: A Comparative Study with Trisacryl-Gelatin Microspheres in the Sheep Model, *J. Vasc. Interventional Radiol.*, 2014, **25**, 1759–1766, DOI: [10.1016/j.jvir.2014.06.025](https://doi.org/10.1016/j.jvir.2014.06.025).
- 42 E. Larrañeta, S. Stewart, M. Ervine, R. Al-Kasasbeh and R. Donnelly, Hydrogels for Hydrophobic Drug Delivery. Classification, Synthesis and Applications, *J. Funct. Biomater.*, 2018, **9**, 13, DOI: [10.3390/jfb9010013](https://doi.org/10.3390/jfb9010013).
- 43 S. H. Ahmad Shariff, R. Daik, M. S. Haris and M. W. Ismail, Hydrophobic Drug Carrier from Polycaprolactone-*b*-Poly(Ethylene Glycol) Star-Shaped Polymers Hydrogel Blend as Potential for Wound Healing Application, *Polymers*, 2023, **15**, 2072, DOI: [10.3390/polym15092072](https://doi.org/10.3390/polym15092072).
- 44 M. F. Meek and K. Jansen, Two years after *in vivo* implantation of poly(DL-lactide- ϵ -caprolactone) nerve guides: Has the material finally resorbed?, *J. Biomed. Mater. Res., Part A*, 2009, **89A**, 734–738, DOI: [10.1002/jbm.a.32024](https://doi.org/10.1002/jbm.a.32024).
- 45 A. J. Haertel, M. A. Schultz, L. M. Colgin and A. L. Johnson, Predictors of Subcutaneous Injection Site Reactions to Sustained-Release Buprenorphine in Rhesus Macaques (*Macaca mulatta*), *J. Am. Assoc. Lab. Anim. Sci.*, 2021, **60**, 329–336.
- 46 Y. Wang, M. Gupta, T. Poonawala, M. Farooqui, Y. Li, F. Peng, S. Rao, M. Ansonoff, J. E. Pintar and K. Gupta, Opioids and opioid receptors orchestrate wound repair, *Transl. Res.*, 2017, **185**, 13–23, DOI: [10.1016/j.trsl.2017.05.003](https://doi.org/10.1016/j.trsl.2017.05.003).
- 47 Y. Wang, A. Otte, H. Park and K. Park, In vitro-in vivo correlation (IVIVC) development for long-acting injectable drug products based on poly(lactide-co-glycolide), *J. Controlled Release*, 2025, **377**, 186–196, DOI: [10.1016/j.jconrel.2024.11.021](https://doi.org/10.1016/j.jconrel.2024.11.021).
- 48 F. Ikomi, Y. Kawai and T. Ohhashi, Recent advance in lymph dynamic analysis in lymphatics and lymph nodes, *Ann. Vasc. Dis.*, 2012, **5**(3), 258–268, DOI: [10.3400/avd.ra.12.00046](https://doi.org/10.3400/avd.ra.12.00046).
- 49 D. Negrini and A. Moriondo, Lymphatic anatomy and biomechanics, *J. Physiol.*, 2011, **589**(Pt 12), 2927–2934, DOI: [10.1113/jphysiol.2011.206672](https://doi.org/10.1113/jphysiol.2011.206672).
- 50 S. Yu, X. Zhang, Y. Sun, Y. Peng, J. Johnson, T. Mandrell, A. J. Shukla and S. C. Laizure, Pharmacokinetics of buprenorphine after intravenous administration in the mouse, *J. Am. Assoc. Lab. Anim. Sci.*, 2006, **45**, 12–16.
- 51 Q. Cai, J. Bei and S. Wang, Synthesis and degradation of a tri-component copolymer derived from glycolide, L-lactide, and ϵ -caprolactone, *J. Biomater. Sci., Polym. Ed.*, 2000, **11**, 273–288, DOI: [10.1163/156856200743698](https://doi.org/10.1163/156856200743698).
- 52 H. Qian, J. Bei and S. Wang, Synthesis, characterization and degradation of ABA block copolymer of L-lactide and ϵ -caprolactone, *Polym. Degrad. Stab.*, 2000, **68**, 423–429, DOI: [10.1016/S0141-3910\(00\)00031-8](https://doi.org/10.1016/S0141-3910(00)00031-8).
- 53 L. Bédouet, F. Pascale, L. Moine, M. Wassef, S. H. Ghegediban, V. N. Nguyen, M. Bonneau, D. Labarre and A. Laurent, Intra-articular fate of degradable poly(ethyleneglycol)-hydrogel microspheres as carriers for sustained drug delivery, *Int. J. Pharm.*, 2013, **456**(2), 536–544, DOI: [10.1016/j.ijpharm.2013.08.016](https://doi.org/10.1016/j.ijpharm.2013.08.016).
- 54 S. Maximos, É. Vaillancourt-Jean, S. Mouksassi, A. De Cassai, S. Ayoub, M. Ruel, J. Desroches, P. O. Hétu, A. Moore and S. Williams, Peak plasma concentration of total and free bupivacaine after erector spinae plane and pectorintercostal fascial plane blocks, *Can. J. Anaesth.*, 2022, **69**(9), 1151–1159, DOI: [10.1007/s12630-022-02260-x](https://doi.org/10.1007/s12630-022-02260-x).
- 55 J. Feng, S. Lepetre-Mouelhi, A. Gautier, S. Mura, C. Cailleau, F. Coudore, M. Hamon and P. Couvreur, A new painkiller nanomedicine to bypass the blood-brain barrier and the use of morphine, *Sci. Adv.*, 2019, **5**(2), eaau5148, DOI: [10.1126/sciadv.aau5148](https://doi.org/10.1126/sciadv.aau5148).
- 56 S. Hua and P. J. Cabot, Targeted nanoparticles that mimic immune cells in pain control inducing analgesic and anti-inflammatory actions: a potential novel treatment of acute and chronic pain condition, *Pain Physician*, 2013, **16**(3), E199–E216.
- 57 C. Stein, Effects of pH on opioid receptor activation and implications for drug design, *Biophys. J.*, 2024, **123**(24), 4158–4166, DOI: [10.1016/j.bpj.2024.07.007](https://doi.org/10.1016/j.bpj.2024.07.007).
- 58 G. T. Whiteside, J. Harrison, J. Boulet, L. Mark, M. Pearson, S. Gottshall and K. Walker, Pharmacological characterisation of a rat model of incisional pain, *Br. J. Pharmacol.*, 2004, **141**, 85–91, DOI: [10.1038/sj.bjp.0705568](https://doi.org/10.1038/sj.bjp.0705568).
- 59 D. Castel, E. Willentz, O. Doron, O. Brenner and S. Meilin, Characterization of a porcine model of post-operative pain, *Eur. J. Pain*, 2014, **18**, 496–505, DOI: [10.1002/j.1532-2149.2013.00399.x](https://doi.org/10.1002/j.1532-2149.2013.00399.x).
- 60 D. Castel, A. Schauder, I. Aizenberg and S. Meilin, Validation of a Gottingen Minipig Model of Post-Operative Incisional Pain, *J. Anesth. Surg. Care*, 2021, **2**, 1–13, DOI: [10.17303/jasc.2021.2.101](https://doi.org/10.17303/jasc.2021.2.101).

